A quality-based approach for radar rain field reconstruction and the H-SAF precipitation products validation


Gianfranco Vulpiani

Gianfranco Vulpiani[1], Angelo Rinollo[1], Silvia Puca[1], and Mario Montopoli[2]

[1]*Dept. of Civil Protection, via Vitorchiano 2, Rome*
[2]*Dept. of of Information Engineering, Sapienza University of Rome, via Eudossiana 18, Rome*
(Dated: 24th July 2014)

1. Introduction

The rainfall product validation program established within the EUMETSAT Satellite Application Facility on Support to Operational Hydrology and Water Management (H-SAF) makes use of the radar and rain gauge observations available among the partner countries (Puca et al., 2014). The H-SAF precipitation products considered in this work are based on the combination of infrared/passive microwave measurements in which the passive microwave precipitation estimates are used in conjunction with SEVIRI images from the geostationary MSG satellite (Mugnai et al., 2013). The intrinsic uncertainties related to the radar rainfall estimation and the network heterogeneity encouraged the design and implementation of a common approach for the radar data quality evaluation to be used as constraint within the validation process. A data quality scheme was recently proposed (Rinollo et al., 2013) to deal with the main error sources, i.e., clutter, partial beam blocking, attenuation, vertical variability of precipitation. In that work, the validation of the PR-OBS-3 (blended IR-MW instantaneous rainfall estimation) product, using radar-based rainfall estimations as ground reference, has shown relevant sensitivity to the estimated radar data quality, encouraging further investigation. The estimate of the radar data quality may play a relevant role either for independent product validation or for data assimilation purposes or for radar rainfall estimation itself (Tabary, 2007). Considering that many of the systems concurring to the Italian radar network have recently acquired dual-polarization capability, it was conceived a new polarimetric processing technique with embedded data quality scheme. Here, it is evaluated using the observations of the rain gauge network as benchmark. Future works will be devoted to the validation of the H-SAF cumulated precipitation product by means of the quality-based radar precipitation fields. This work first summarize the recent findings of Rinollo et al. (2013), then describes and validate the considered radar processing chain.

2. The H-SAF blending precipitation product PR-OBS-3

The standard PR-OBS-3 algorithm combines the temporally-rich information from the SEVIRI infrared (IR) geostationary observations together with the more quantitative, but less frequent, rainfall information from the passive microwave polar orbiting satellites (i.e. H-SAF from the products PR-OBS-1 and PR-OBS-2). The infrared and PMW observations are blended using the probability matching technique. The probability matching approach used for PR-OBS-3 was originally developed at the US Naval Research Laboratory (NRL) and therefore it is referred to as NRL Technique (NRLT). The NRLT processing is triggered as soon as a new slot of SEVIRI data at $10.8\,\mu m$ is available. As a second step, the identification of the PMW measurements coincident in time and space with the TBs at $10.8\,\mu m$ of the currently processed SEVIRI image is performed. The coincident data are subsequently located in a geographical latitude/longitude grid, and for each grid box the histogram of the IR BTs and that of the corresponding PMW rain rates are built and then combined by means of a probabilistic histogram matching technique (Calheiros and Zawadzki, 1987) to produce geo-located IR-BT vs. PMW rain-rate relationships. These relationships are then used to assign a rainfall intensity value to each SEVIRI pixel. As soon as a grid box is refreshed with new data, the corresponding relationship is renewed using updated IR-TB and PMW rain-rate histograms. Relationships older than 24 h with respect to the acquisition time of the IR BT are considered unreliable and consequently no rainfall intensity values are assigned until a refresh of the relationship is done.

The key point of this technique is thus to provide instantaneous rainfall estimations at the GEO spatial and temporal scales, which are consistent with the nature and development of the precipitating cloud systems, by overcoming the scarcity of PMW overpasses with the more frequent GEO slots and the weak connection between the rain intensity and IR BTs with the calibration of the IR BTs by the PMW rain rates. Note that in order to apply the IR-PMW blending, PR-OBS1 or PR-OBS2 or both can be used to feed the PR-OBS3 algorithm.

In Rinollo et al. (2013) 12 rainfall events occurred in central Italy and observed by the radar system located in Tufillo (Chieti) near the Adriatic coastline have been considered. The validation of the PR-OBS-3 has shown a remarkable sensitivity with respect to radar data quality used to filter out the precipitation pixels with limited reliability. Indeed as shonwn in Fig. 1, the relative RMSE (defined as the ratio between RMSE and the reference rainfall) decreases at increasing radar data quality thresholds either on sea or on land.

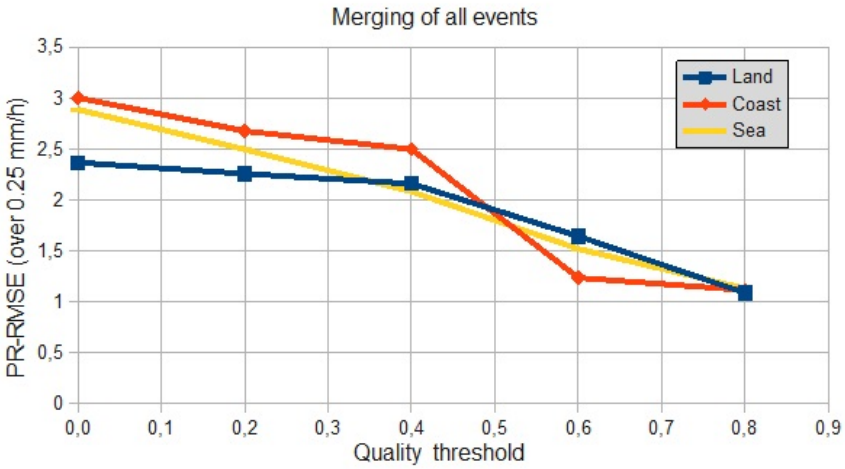

Figure 1: Sensitivity of the PR-OBS-3 accuracy with respect to radar data quality.

3. Radar data processing scheme

The operational radar processing chain, currently under testing within the H-SAF project, is briefly described in this section. It aims at compensating or at least identifying most of the uncertainty sources conditioning the radar rainfall estimation process (Friedrich et al., 2006). Among them, the following error sources are primarily considered: contamination by non-weather resturns (clutter), Partial Beam Blocking (PBB), beam broadening at increasing distances, vertical variability of precipitation (Germann and Joss, 2002; Joss and Lee, 1995; Marzano et al., 2004) and rain path attenuation (Bringi and Chandrasekar, 2001; Carey et al., 2000; Testud et al., 2000; Vulpiani et al., 2008). Every error source is quantified through specific tests ending with the estimation of specific (partial) quality matrices and, when possibile, is compensated for. The overall data quality (Q) is then obtained as a combination of the partial quality matrices. The quality model described in Rinollo et al. (2013) is embedded within the overall processing chain schematically depicted in Figure 1. In this schematic representation, the sequential flow among consecutive computational steps is specified by black arrows, while the blue ones identify the data input (or output) to (or from) a specific processing module.

The processing chain can be summarized through the following few steps as follows:

i. As typical, the raw volumetric data must be first filtered from non-weather returns. This step is here achieved using the fuzzy-logic approach proposed in Vulpiani et al. (2012) for polarimetric radar systems.

ii. The next step is the correction for Partial Beam Blocking (PBB) based on the retrieved 3-D conclusion map (Bech et al., 2003) that, assuming the e.m. waves propagate in a standard atmosphere, is evaluated only once for a given radar scanning strategy.

iii. The rain path attenuation is just qualitatively evaluated in case the considered radar system has single-polarization capability (Rinollo et al., 2013), otherwise it is compensated for by means of the differential phase shift that needs to be preliminarly processed. In this framework, the iterative moving-window range derivative approach proposed in Vulpiani et al. (2012) is applied here. This methodology enables, on one side, to easily remove the offset on Φ_{DP}, facilitating the application of any attenuation correction procedures, and, on the other side, to control the expected K_{DP} standard deviation, expressible as follows

$$\sigma(K_{DP}^{(I)}) = \frac{1}{\sqrt{2\,N^I}} \frac{\sigma(\Psi_{DP})}{L} \tag{3.1}$$

where I is the number of iterations (with $I \geq 1$), N the number of range gates contained in the moving window of length L (km), and Ψ_{DP} is the measured differential phase, i.e., the sum of the differential propagation (Φ_{DP}) and backscatter phase (δ_{HV}).

iv. The range-related deterioration of radar data quality is modeled through a non-linear function as in Rinollo et al. (2013).

v. Once the attenuation is evaluated and, eventually, compensated for through the so-called ZPHI method (Testud et al., 2000), the overall data quality is computed as geometric mean of the partial quality matrices.

$$Q = q_{clutter} \times q_{vertical} \times q_{PBB} \times q_{distance} \times q_{attenuation} \tag{3.2}$$

vi. The retrieved mean Vertical Profile of Reflectivity (VPR) is applied to the entire volumetric scan with the aim to use all

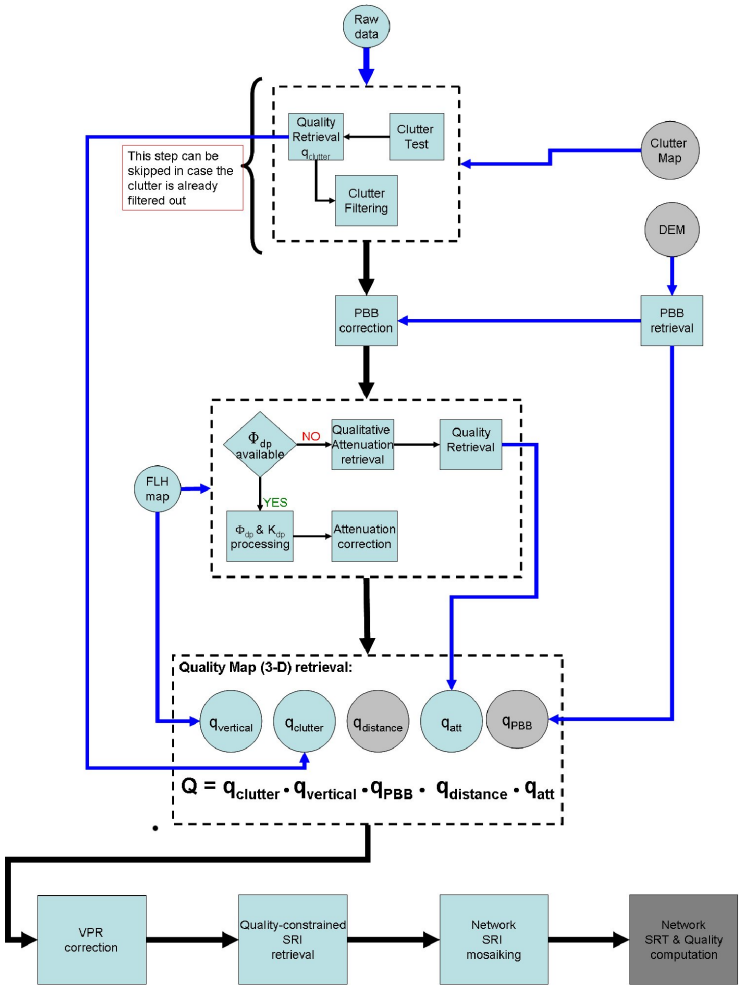

Figure 2: Block diagram showing the radar data processing chain, including the computation of the data quality.

the observations along the vertical to retrieve the surface rainfall rate.

All the clutter-filtered and attenuation-corrected (if applicable) PPIs are projected at ground by means of the average Vertical Profile of Reflectivity (VPR). In such a way we get N_{sweeps} 2-D fields of ground-equivalent observations, N_{sweeps} being the number of sweeps or PPIs. Denoting with $Z_{cil} = Z(\rho, \phi, h)$ the reflectivity volume resampled in a cylindrical coordinate system, the ground projection is accomplished by the functional f_{VPR}

$$Z(\rho, \phi, h_g) = f_{VPR}\left(Z(\rho, \phi, h)\right) = Z(\rho, \phi, h) - \Delta Z \tag{3.3}$$

where $\Delta Z = \eta_{dB}(h) - \eta_{dB}(h_g)$, η_{dB} being the decibel conversion of the mean VPR obtained as spatial average of $Z(\rho, \phi, h)$ (expressed in linear units)

$$\eta(h) = \frac{\sum_{k=1}^{N_{range}} \sum_{j=1}^{N_{azim}} Z(\rho_k, \phi_j, h)}{N_{range}\, N_{azim}} \tag{3.4}$$

where N_{range} and N_{azim} are the number of sampled range gates and azimuth, respectively. It is worth specifying that the VPR correction is not applied during the summer season.

vii. The Surface Rainfall Intensity (SRI) map is computed as a quality-weighted average of each rain rate map, obtained by each ground-projected reflectivity sweep. Every single-radar surface rainfall intensity map is computed as a quality-weighted average of each rain rate map R_{sweep}, obtained by each ground-projected reflectivity sweep:

$$R_Z(r, \phi, h_g) = \frac{\sum_{k=1}^{N_{sweeps}} Q\left(r, \phi, h_k\right) R_{sweep}\left(r, \phi, h_{g,k}\right)}{\sum_{k=1}^{N_{sweeps}} Q\left(r, \phi, h_k\right)} \tag{3.5}$$

where

$$R_{sweep}\left(r, \phi, h_{g,k}\right) = a_Z \left[f_{VPR}\left(Z\left(r, \phi, \theta_k\right)\right)\right]^{b_Z} \tag{3.6}$$

with $a_Z = 0.0365$ and $b_Z = 0.6250$ (Marshall and Palmer, 1948), k ranging from 1 to N_{sweeps}.

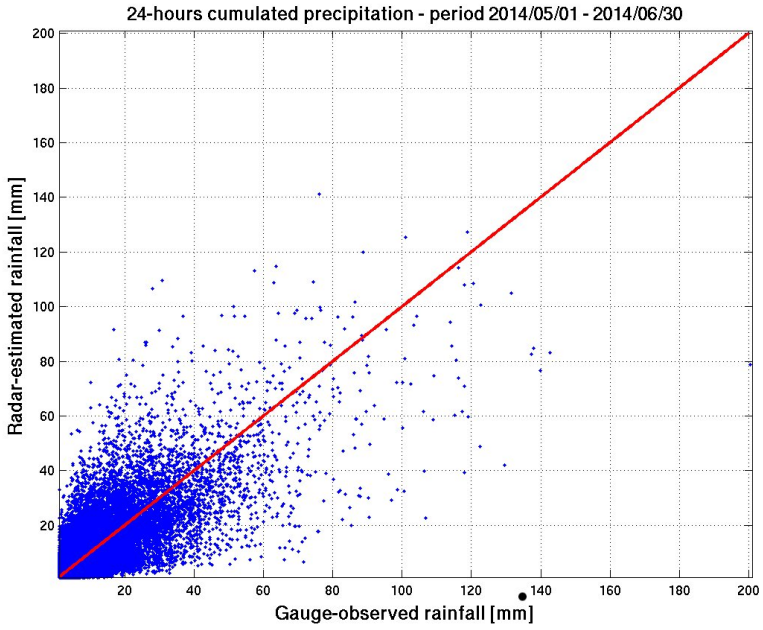

Figure 3: Radar versus gauge 24-h cumulated precipitation during the period 01 May - 30 June 2014.

In case of dual-polarization systems, the composite rainfall retrieval algorithm proposed in Vulpiani and Baldini (2013) is applied

$$R_c = w_K \cdot R_K + (1 - w_K) \cdot R_Z \tag{3.7}$$

where

$$R_K\left(r, \phi\right) = a_K \left[f_{LBM}\left(K_{DP}\right)\right]^{b_K} \tag{3.8}$$

with $a_K = 24.68$, $b_K = 0.81$ at C-band (Bringi et al., 2011) , f_{LBM} is the functional computing the Lowest Beam Map (LBM), whereas the weight w_K is defined as

$$w_K = \begin{cases} 0, & \text{if } K_{dp} \leq 0.5 \\ 2 \cdot K_{dp} - 1, & \text{if } 0.5 < K_{dp} < 1 \\ 1, & \text{if } K_{dp} \geq 1 \end{cases} \tag{3.9}$$

The error structure of K_{dp} is generally different from the reflectivity one, even though there are common elements. They both suffer for the contamination by non-weather returns. Despite K_{dp} is immune to attenuation, the range-related errors, such as beam broadening and, consequently, non-uniform beam filling, do affect specific differential phase too. However, because K_{dp} is immune to partial beam blocking the lower tilts can be used more to estimate precipitation. Because K_{dp} is an estimated quantity sensitive to noise, it is commonly considered reliable for values higher than its expected standard deviation (it is assumed an unbiased estimate), i.e., a few tens of $deg\, km^{-1}$, depending on the radar system and phase processing technique. Within this work, it is assumed that once the clutter is removed the quality of K_{dp} is only related to its estimation procedure. Future works will be devoted to take into account its vertical variability and the non-uniform beam filling.

viii. The SRI composite is built by combining the single-radar rainfall maps through a squared-quality-weighted approach.

3.1. SRI and SRT composite

The network SRI (SRI_{comp}) is computed adopting highest-quality mosaiking criterium, i.e., in a given geographical position covered by two or more radars, the single-radar SRI with the highest quality is considered. The quality of SRI_{comp} is then obtained by averaging the single-radar quality matrices $Q_{SRI_{comp}} = mean\{Q_j\}$. The Surface Rainfall Total (SRT) or cumulated rainfall is obtained by integrating SRI_{comp}, while the quality of SRT (denoted as Q_{SRT}) is obtained by averaging $Q_{SRI_{comp}}$.

Table 1: Statistical performance of the radar rainfall estimation algorithm for different cumualtion intervals.

Time	1 h	3 h	6 h	12 h	24 h
$RMSE$	2.88	4.05	4.87	5.73	6.90
σ_ε	2.88	4.03	4.86	5.71	6.87
$\langle\varepsilon\rangle$	-0.17	-0.30	-0.40	-0.50	-0.64
MAE	1.34	1.95	2.40	2.91	3.61
$Bias$	0.93	0.93	0.92	0.92	0.93
cc	0.74	0.79	0.81	0.82	0.83

3.2. Radar rainfall assessment

The radar rainfall algorithm described above is running operationally since the end of April 2014, consequently the performance analysis, carried out for the time being, cannot be exaustive. Notwithstanding, the considered algorithm performed reasonably well during the reference period (i.e., 1st May - 30 June 2014) as it can be argued by Figure 3 showing the distribution of the estimated versus observed 24-h cumulated precipitation. As it can be noticed, the distribution is relatively simmetric with respect to the bisector even though with a non-negligible dispersion. The quantitative performance analysis has been carried out using several error indicators, i.e. root mean square error $RMSE$, the error standard deviation σ_ε, the mean error $\langle\varepsilon\rangle$, the mean absolute error MAE, the multiplicative bias $Bias = \frac{\langle R_{RADAR}\rangle}{\langle R_{GAUGES}\rangle}$, the correlation coefficient cc, where $\langle\cdot\rangle$ stands for the average operator.

According to Tab. 1 summarizing the error scores referred to different cumulation intervals, the accuracy is relatively high in terms of Bias, MAE and correlation coefficient. As expected most of the RMSE is related to the error standard deviation, the mean error being relatively low. As already mentioned the results of the present analysis are very preliminary, having been perfomed only on

4. Conclusions

A radar processing chain with embedded quality scheme was developed within the H-SAF project with the aim to provide a relatively reliable benchmarlk for the validation if satellite-based rainfall products obtained by the combination of infrared and microwave observation. The radar processing chain tested on operational conditions in Italy during may and june 2014 has shown a relatively good perfomance in terms of mean bias even for short cumulation time, even though the error standard deviation is relevant. Due to the complex orography scenario, it is expected a remarkable performance deterioration during the fall-winter season when the lowering of the freezing layer increases the contamination by ice and/or melting particles. Future works will be devoted to the validation of the satellite-based precipitation products developed within the H-SAF project context using quality-controlled radar precipitation fields on national scale.

References

Bech, J., B. Codina, J. Lorente, and D. Bebbington, 2003: The sensitivity of single polarization weather radar beam blockage correction to variability in the vertical refractivity gradient. *J. Atmos. Oceanic Technol.*, **20**, 845–855.

Bringi, V. N. and V. Chandrasekar, 2001: *Polarimetric doppler weather radar*. Cambridge University Press, 636 pp.

Bringi, V. N., M. Rico-Ramirez, and M. Thurai, 2011: Rainfall estimation with an operational polarimetric c-band radar in the united kingdom: comparison with a gauge network and error analysis. *J. Hydrometeor.*, **12**, 935–954.

Carey, L. D., S. A. Rutledge, and D. A. Ahijevych, 2000: Correcting propagation effects in c-band polarimetric radar observations of tropical convection using differential propagation phase. *J. Appl. Meteor.*, **39**, 1405–1433.

Friedrich, K., M. Hagen, and T. Einfalt, 2006: A quality control concept for radar reflectivity, polarimetric parameters, and doppler velocity. *J. Atmos. Ocean. Tech.*, **23**, 865–887.

Germann, U. and J. Joss, 2002: Mesobeta profiles to extrapolate radar precipitation measurements above the alps to the ground level. *J. Appl. Meteorol.*, **41**, 542–557.

Joss, J. and R. Lee, 1995: The application of radar-gauge comparisons to operational precipitation profile corrections. *J. Appl. Meteorol.*, **34**, 2612–2630.

Marshall, J. S. and W. M. Palmer, 1948: The distribution of raindrops with size. *J. Meteor.*, **5**, 165–166.

Marzano, F. S., G. Vulpiani, and E. Picciotti, 2004: Rain field and reflectivity vertical profile reconstruction from c-band radar volumetric data. *IEEE Trans. Geosci. Rem. Sens.*, **42**, 1033–1046.

Mugnai, A., et al., 2013: Precipitation products from the hydrology saf. *Nat. Hazards Earth Syst. Sci.*, **13**, 1959–1981.

Puca, S., et al., 2014: The validation service of the hydrological saf geostationary and polar satellite precipitation products. *Nat. Hazards Earth Syst. Sci.*, **14**, 871–889.

Rinollo, A., et al., 2013: Definition and impact of a quality index for radar-based reference measurements in the h-saf precipitation product validation. *Nat. Hazards Earth Syst. Sci.*, **13**, 1–11.

Tabary, P., 2007: The new french operational radar rainfall product. part i: methodology. *Wea. Forecasting*, **22**, 393–408.

Testud, J., E. L. Bouar, E. Obligis, , and M. Ali-Mehenni, 2000: The rain profiling algorithm applied to polarimetric weather radar. *J. Atmos. Oceanic Technol.*, **17**, 332–356.

Vulpiani, G. and L. Baldini, 2013: Observations of a severe hail-bearing storm by an operational X-band polarimetric radar in the mediterranean area. *Proceed. of the 36th AMS Conference on Radar Meteorology, Breckenridge, CO, USA*.

Vulpiani, G., M. Montopoli, L. D. Passeri, A. Gioia, P. Giordano, and F. S. Marzano, 2012: On the use of dual-polarized C-band radar for operational rainfall retrieval in mountainous areas. *J. Appl. Meteor and Clim.*, **51**, 405–425.

Vulpiani, G., P. Tabary, J. P. D. Chatelet, and F. S. Marzano, 2008: Comparison of advanced radar polarimetric techniques for operational attenuation correction at c band. *J. Atmos. Oceanic Technol.*, **25**, 1118–1135.